

**MODIFICATIONS OF LAYERED SILICATES AND LAYERED DOUBLE
HYDROXIDES FOR PREPARATION OF POLYOLEFIN
NANOCOMPOSITES**

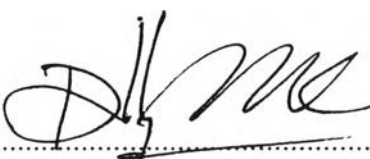
Nattaya Muksing

A Dissertation Submitted in Partial Fulfilment of the Requirements
for the Degree of Doctor of Philosophy
The Petroleum and Petrochemical College, Chulalongkorn University
in Academic Partnership with
The University of Michigan, The University of Oklahoma,
and Case Western Reserve University

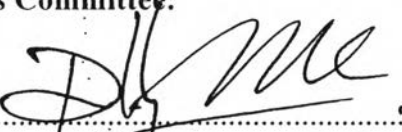
2011


Thesis Title: Modification of Layered Silicates and Layered Double Hydroxides for Preparation of Polyolefins Nanocomposites.
By: Nattaya Muksing
Program: Polymer Science
Thesis Advisors: Assoc. Prof. Ratanawan Magaraphan
Asst. Prof. Manit Nithitanakul
Prof. Brian P. Grady
Dr. Elisa Passaglia
Prof. Francesco Ciardelli

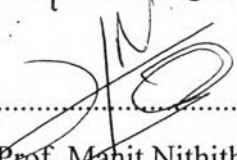
Accepted by the Petroleum and Petrochemical College, Chulalongkorn University, in partial fulfilment of the requirements for the Degree of Doctor of Philosophy.

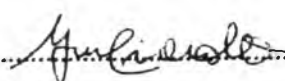

..... Dean
(Asst. Prof. Pomthong Malakul)

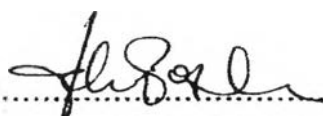
Thesis Committee:

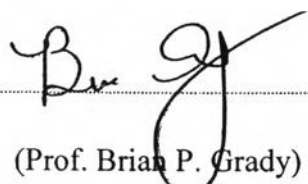

.....
(Asst. Prof. Pomthong Malakul)



.....
(Assoc. Prof. Rathanawan Magaraphan)

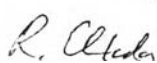

.....
(Asst. Prof. Manit Nithithanakul)


.....
(Prof. Francesco Ciardelli)


.....
(Dr. Elisa Passaglia)


.....
(Prof. Brian P. Grady)


.....
(Asst. Prof. Hathaikhan Manuspiya)


.....
(Asst. Prof. Chonlada Ritvirulh)

บทคัดย่อ

นาคยา มัคสิงห์ : การดัดแปรสภาพขั้วของแร่ดินเหนียว ชนิด เลเซอร์ซิลิเกต และเลเซอร์ดับเบิลไฮดรอกไซด์ เพื่อนำไปใช้ในการเตรียมนาโนคอมโพสิตของพอลิโอเลฟินส์ (Modifications of Layered Silicates and Layered Double Hydroxides for Preparation of Polyolefins Nanocomposites) อ. ที่ปรึกษา : รศ.ดร. รัตนวรรณ มกรพันธุ์ ผศ. ดร. มานิตย์ นิธิธนากุล ศ. ดร. ฟราสเชสโก ซาเคลลี ศ. ดร. ไบรอัน เกรดี และ ดร. เอลิซา พาสเกลีย 206 หน้า

ในวิทยานิพนธ์เล่มนี้ แร่ดินเหนียวชนิดแผ่นบาง (เลเซอร์ เคลย์) สองชนิด คือ ซิลิเกตเคลย์ และ ดับเบิลไฮดรอกไซด์ เคลย์ ถูกนำมาใช้เป็นสารเสริมแรงในการเตรียมนาโนคอมโพสิตสำหรับพอลิพรอพิลีน และพอลิเอทิลีน ตามลำดับ นาโนคอมโพสิตทั้งสองชนิดถูกเตรียมโดยใช้เทคนิคการผสมแบบสภาวะหลอมเหลว โดยใช้เครื่องอัดรีดแบบสกรูคู่ และมีพอลิโอเลฟินส์กราฟมาเลอิกแอนไฮไดรด์ ทำหน้าที่เป็นตัวเชื่อมประสานระหว่างแร่ดินเหนียวและพอลิเมอร์ สำหรับพอลิพรอพิลีน/ซิลิเกต เคลย์ นาโนคอมโพสิต แร่ดินเหนียวนั้นถูกนำมาดัดแปลงสภาพผิวโดยใช้สารลดแรงตึงผิวแบบประจุบวกชนิดต่างๆ เพื่อให้ได้แร่ดินเหนียวที่เรียกว่าออร์กาโนเคลย์ จากผลการวิจัยพบว่านาโนคอมโพสิตที่เตรียมได้จากการใช้สารลดแรงตึงผิวแบบประจุบวกชนิดที่มีสายโซ่ยาวนั้นให้นาโนคอมโพสิตที่มีสมบัติที่ดี โครงสร้างของนาโนคอมโพสิตที่เตรียมได้นั้นสามารถแบ่งเป็นสองกลุ่มที่ชัดเจน คือ แบบเอกโฟลิเอทบางส่วน และแบบอินเตอร์คาเลท และพบว่าโครงสร้างแบบผสมของอินเตอร์คาเลทและเอกโฟลิเอทนั้นจะปรากฏให้เห็นเมื่อความเข้มข้นของออร์กาโนเคลย์มากกว่า 3 เปอร์เซ็นต์โดยน้ำหนัก โครงสร้างนาโนคอมโพสิตแบบอินเตอร์คาเลท หรือเอกโฟลิเอทที่แตกต่างกันส่งผลให้สมบัติทางความร้อนแตกต่างกันด้วย การเพิ่มขึ้นของอุณหภูมิการเปลี่ยนจากสถานะคล้ายแก้วนั้นเป็นผลมาจากสายโซ่พอลิเมอร์ถูกจำกัดอยู่ระหว่างชั้นของเลเซอร์เคลย์ สำหรับกรณีพอลิเอทิลีนชนิดความหนาแน่นต่ำ/ดับเบิลไฮดรอกไซด์เคลย์ นาโนคอมโพสิตนั้น ดับเบิลไฮดรอกไซด์ เคลย์ ถูกนำมาดัดแปลงสภาพผิวเช่นเดียวกันโดยใช้สารลดแรงตึงผิวแบบประจุลบชนิดต่างๆ จากผลการวิจัยพบว่าขนาดหรือโครงสร้างของสารลดแรงตึงผิวนั้นมีความสำคัญอย่างมากต่อโครงสร้างและสมบัติทางความร้อนของนาโนคอมโพสิตนาโนคอมโพสิตที่ได้เป็นแบบผสมระหว่างอินเตอร์คาเลทและเอกโฟลิเอท และพบว่าสารลดแรงตึงผิวชนิดสายโซ่ยาวตั้งแต่ 12 สายขึ้นไปเหมาะสมที่สุดที่จะนำมาใช้ในการเตรียมนาโนคอมโพสิต นอกจากนั้นพบว่า การเติมออร์กาโนเคลย์ลงไปในพอลิเมอร์นั้นช่วยปรับปรุงทั้งสมบัติทางความร้อนและสมบัติสมบัติพลวัตเชิงกลอีกด้วย

ABSTRACT

4782004063: Polymer Science Program

Nattaya Muksing: Modifications of Layered Silicates and Layered Double Hydroxides for Preparation of Polyolefins Nanocomposites.

Thesis Advisor: Assoc. Prof. Ratanawan Magaraphan, Prof.

Francesco Ciardelli and Asst. Prof. Manit Nithithanakun 206 pp.

Keywords: Layered silicate/ Layered double hydroxide/ Melt intercalation/ Organoclay/ Polypropylene/ Polyethylene/ Nanocomposite

In this dissertation, two types of layered inorganic clays: layered silicate and layered double hydroxide (LDH) were chosen as nanofillers for the preparation of polyolefins nanocomposites. Both types of nanocomposites were prepared by melt intercalation technique using a twin screw extruder. The polyolefins grafted maleic anhydride (i.e. PP-g-MAH and PE-g-MAH) were used as the compatibilizer. For polypropylene/layered silicate nanocomposites, the clay was modified with various cationic surfactants to obtain the organoclay. The nanocomposites prepared from organoclay that modified by the longer alkyl chain length surfactant, showed a good property. Two distinct groups of the nanocomposites, from a quasi-exfoliated to an intercalated morphology, were identified. The intercalated/flocculated morphologies were obtained when the organoclay content beyond 3 wt%. The different degrees of exfoliation/intercalation revealed the variable increase in thermal stability of the nanocomposites. The increase in glass transition temperature was related to the confinement effect between the polymer chains and the clay layers. For low density polyethylene/layered double hydroxide (LDH) nanocomposites, the LDH-clay was modified by various anionic surfactants. The result revealed that the size of the anionic surfactants played a vital role for the difference in morphological and thermal property. The obtained nanocomposites established partially exfoliated/intercalated mixed morphology and were preferable when the number of alkyl chain length was larger ($n \geq 12$). Incorporation of the organoclay enhanced both thermal and dynamic mechanical properties (i.e. storage modulus and glass transition temperature).

ACKNOWLEDGEMENTS

Appreciation is expressed to those who have made contributions to this dissertation. First the author gratefully acknowledges her advisor, Assoc. Prof. Rathanawan Magaraphan and Asst. Prof. Manit Nithitanakul for giving her invaluable knowledge, meaningful guidance and beneficial encouragement all along the way.

She also would like to express her sincere thanks to Prof. Francesco Ciardelli, Dr. Elisa Passaglia and Dr. Serena Coiai for giving her useful advises and suggestions as well as their kind taking care while she did a part of her research at Department of Chemistry and Industrial Chemistry, University of Pisa.

She would like also to express her sincere thanks to Prof. Brian P. Grady from University of Oklahoma for giving her useful comments and suggestions and helping her some SAXD and DSC analysis of her materials.

She gratefully acknowledges all faculty members and staffs at The Petroleum and Petrochemical College, Chulalongkorn University for their knowledge and assistance. Moreover, she would like to give her special thanks to all members in her research group both from the Petroleum and Petrochemical College, Chulalongkorn University and from Department of Chemistry and Industrial Chemistry, University of Pisa, as well as all of her friends for their help and supports.

She would like also to express her sincere thanks to Asst. Prof. Pomthong Malakul, Asst. Prof. Hathaikarn Manuspiya, and Asst. Prof. Chonlada Ritvirulh for being her dissertation committees, making valuable comments and suggestions.

She wishes to express her deep gratitude to her family for their unconditioned love, understanding and very supportive during all these years spent for her Ph.D. study.

Finally, the author is deeply indebted to the Royal Golden Jubilee Ph.D Program (RGJ) for providing a full scholarship as well as encouragement for doing a part of research work in Italy, and partial fund from National Center of Excellence for Petroleum, Petrochemicals, and Advanced Materials and University of Pisa. This work would not be carried out successfully without all financial supports.

TABLE OF CONTENTS

	PAGE
Title Page	i
Abstract (in English)	iii
Abstract (in Thai)	iv
Acknowledgements	v
Table of Contents	vi
List of Tables	ix
List of Figures	xi
Abbreviations	xviii
 CHAPTER	
I INTRODUCTION	1
II LITERATURE REVIEW	5
III EXPERIMENTAL	53
IV EFFECT OF ORGANOCCLAYS DISPERSION ON MORPHOLOGY, THERMAL, CRYSTALLIZATION AND MECHANICAL PROPERTIES OF POLYPROPYLENE/ LAYERED SILICATE NANOCOMPOSITES	71
4.1 Abstract	71
4.2 Introduction	72
4.3 Results and Discussion	75
4.4 Conclusions	93

CHAPTER		PAGE
V	MORPHOLOGY DEVELOPMENT AND STABILITY OF POLYPROPYLENE/ORGANOCLAY NANOCOMPOSITES	94
	5.1 Abstract	94
	5.2 Introduction	95
	5.3 Results and Discussion	99
	5.4 Conclusions	117
VI	MELT RHEOLOGY AND EXTRUDATE SWELL OF POLYPROPYLENE/ORGANOBENTONITE-FILLED POLYPROPYLENE NANOCOMPOSITES	118
	6.1 Abstract	118
	6.2 Introduction	118
	6.3 Results and Discussion	122
	6.4 Conclusions	138
VII	ANIONIC SURFACTANTS INTERCALATED LAYERED DOUBLE HYDROXIDES BASED- LOW DENSITY POLYETHYLENE NANOCOMPOSITES	139
	7.1 Abstract	139
	7.2 Introduction	140
	7.3 Results and Discussion	144
	7.4 Conclusions	169

CHAPTER	PAGE
VIII CONCLUSIONS AND RECOMMENDATIONS	171
REFERENCES	174
APPENDICES	196
Appendix A Some Calculations for Layered Clays	196
Appendix B Supplementary Results of Chapter IV	200
Appendix C Supplementary Results of Chapter VII	201
CURRICULUM VITAE	204

LIST OF TABLES

TABLE		PAGE
CHAPTER II		
2.1	Chemical formula and characteristic parameter commonly used 2:1 phyllosilicates	8
CHAPTER III		
3.1	Physical properties of Na-bentonite as compared to Na-montmorillonite	53
3.2	Chemical structure of the cationic surfactants	54
3.3	Chemical structure of the anionic surfactants	55
3.4	Resin properties of polypropylene (PP)	56
3.5	Resin properties of low density polyethylene (LDPE)	56
3.6	Desiging formula for preparing PP/layered silicate nanocomposites	60
3.7	Desiging formula for preparing LDPE/Organo-LDHs nanocomposites	62
CHAPTER IV		
4.1	Swelling power, cation exchange capacity and elemental analysis of Na-Bentonite, Purified Bentonite and Na-Montmorillonite	77
4.2	Chemical structure of alkyl ammonium surfactants and their interlayer spacing after organic modification	81
4.3	The degradation temperature at 10 and 50% weight loss ($T_{10\%}$ and $T_{50\%}$), melting (T_m) crystallization temperature (T_c), melting enthalpy (ΔH_m), % crystallinity (χ_c) of various PP/organoclay nanocomposites	89

TABLE	PAGE
CHAPTER V	
5.1 DSC and TGA results of PP/PPMAH and PP/organoclay nanocomposites at various OBTN content	103
5.2 Xylene and toluene extraction results, % residue, and glass transition temperature of pure PP, PP/PPMAH, and nanocomposites	116
CHAPTER VI	
6.1 Activation energy (E_a) for viscous flow of organobentonite-filled PP nanocomposites at various shear rates	129
6.2 Power law exponent (n) and melt viscosity coefficient (K) of organobentonite-filled PP nanocomposites at various temperatures	130
6.3 The values of α_1 and β_1 for 5 wt% organobentonite-filled PP nanocomposites at various shear rates	137
6.4 The values of melt elasticity constants, B_0 and B_1 for unfilled and organobentonite-filled PP nanocomposites	137
CHAPTER VII	
7.1 The reflections in $\langle 00l \rangle$ series and interlayer spacing for LDH-NO ₃ and the organomodified LDH with different alkyl sulfate surfactants	150
7.2 Designing formula for preparing LDPE/Organomodified LDHs nanocomposites and their thermal properties	163
7.3 Dynamic storage moduli and peak temperature of relaxations for LDPE/organomodified LDHs nanocomposites	166

LIST OF FIGURES

FIGURE	PAGE
CHAPTER II	
2.1	Structure of 2:1 phyllosilicates 7
2.2	X-ray diffraction pattern of Na-montmorillonite showing the (00l) basal reflections (in bold) and the (hk0) diffraction bands. In some cases, both reflections are overlapping 9
2.3	Schematic represents the cation-exchange process between alkylammonium ions and cations (i.e. Na ⁺ , Li ⁺ , Ca ²⁺) situated in the intercalated between the silicate layers 10
2.4	(A) X-ray diffraction patterns of Na-MMT as the length of the alkylammonium chain increases and (B) TEM images of injection molded HMW nylon 6 nanocomposites as different silicate clays: (a) (HE) ₂ M ₁ R ₁ -WY (higher CEC) and (b) (HE) ₂ M ₁ R ₁ -YM (lower CEC) 11
2.5	Schematic of the orientations of alkylammonium ions in the galleries of layered silicates with different layer charge densities 12
2.6	Schematic of different types of composite arising from the interaction of layered silicates and polymers: Conventional composite, Intercalated nanocomposite and Exfoliated nanocomposite 13
2.7	Schematic illustrates the intercalation of polymer or pre-polymer from solution 16
2.8	Schematic illustrates the in-situ intercalative polymerization 17
2.9	Schematic illustrates the melt intercalation 18
2.10	Schematic depicting the intercalation process between a polymer melt and an OMLS 20

FIGURE	PAGE
2.11 Schematic depicting the dispersion process of the organized clay in the PP matrix with the aid of compatibilizer (PP-MA)	21
2.12 (A) XRD patterns of a dimethyldioctadecylammonium-modified montmorillonite (2C18-MMT) and all of the functionalized-PP/2C18-MMT nanocomposites at different functional groups: (a) methylstyrene 1 mol %, (b) maleic anhydride 0.5 mol % and (c) hydroxyl-containing styrene 0.5 mol % and (B) TEM image of the functionalized-PP/2C18-MMT nanocomposite structure (PPr-MA/6 wt % OMMT)	25
2.13 TEM micrographs (X10,000) of PP/PP-g-MA/Cloisite®20A composites with different PP-g-MA content	26
2.14 TEM images of PP/clay hybrids: (a) PP/MAPP/OMT1, (b) PP/MAPP/OMT2 and (c) PP/MAPP/OMT3	26
2.15 Mechanical properties of PPLSNs as a function of clay content	29
2.16 (A) TGA curves of iPP/OMMT hybrids containing various OMMT contents and (B) thermal degradation temperatures (T_d) as a function of OMMT content	32
2.17 Linear melt-state rheological properties as a function of oscillatory frequency: (a) storage modulus (G') and (b) loss modulus (G'')	36
2.18 Schematic Representation comparing the crystal structure of (A) brucite and (B) Layered Double Hydroxide (LDH)	39
2.19 Scheme of Rehydration of calcined LDH precursor	42
2.20 Schematic illustrates the preparation method of polymer/LDH nanocomposites: (A) direct intercalation; (B) in-situ polymerization; (c) in-situ synthesis; (D) exfoliation/restacking and (E) reconstruction	44

FIGURE	PAGE
2.21 (A) XRD spectra, (B) TEM images of HDPE-g-MA/LDH (PBXLDH) nanocomposites with (a) 0.5 phr, (b) 1.0 phr, (c) 2.0 phr and (d) 10 phr and (C) XRD spectra of PE/stearate ZnAl LDH nanocomposites	49
2.22 The tensile properties of polyethylene/LDH nanocomposites comparison with their unfilled matrix	51
CHAPTER III	
3.1 The co-rotating twin screw extruder (Collin) and the operating temperatures of the extruder	59
3.2 The Brabender Plastograph (PL2100) mixer	61
3.3 The CEAST Rheologic 500 twin-bore capillary rheometer	67
CHAPTER IV	
4.1 XRD patterns of Na-bentonite, Purified bentonite and Na-montmorillonite	75
4.2 XRD patterns of the organoclays modified with different alkyl ammonium surfactants	78
4.3 XRD patterns of PP nanocomposite based: (a) CTAB-clay, (b) BTC-clay, and (c) DOEM-clay, for various organoclay contents	79
4.4 Representative TEM micrographs of PP nanocomposite based: (a) CTAB-clay, (b) BTC-clay, and (c) DOEM-clay, for 5wt% organoclay loading	82
4.5 TGA thermograms of PP/organoclay nanocomposites for different types of organoclay (a) CTAB-clay, (b) BTC-clay, and (c) DOEM-clay	85
4.6 Typical peak deconvolution of amorphous and crystalline components of the PP WAXD profile	87

FIGURE	PAGE
4.7 WAXD patterns for different types of PP/orgnoclays: (a) CTAB-clay, (b) BTC-clay, and (c) DOEM-clay	88
4.8 Mechanical properties of different PP/orgnoclays: (a) Tensile strength, (b) Tensile modulus, and (c) %Elongation at break	91
 CHAPTER V 	
5.1 XRD patterns of PP/orgnoclays at various OBTN contents	100
5.2 Crystallization thermograms of PP/orgnoclays at various OBTN contents	101
5.3 DSC thermograms of PP/orgnoclays at various OBTN contents: determination of the glass transition temperature (T_g)	102
5.4 TGA (top) and DTG (bottom) thermograms of PP/orgnoclays at various OBTN contents	104
5.5 FTIR spectra of (a) 7 wt% OBTN nanocomposite xylene-residue, (b) OBTN organoclay, and (c) PP/PPMAH blend	106
5.6 XRD pattern of the 7wt% OBTN nanocomposite xylene-residue fraction	106
5.7 FTIR spectra of the (a) soluble fractions and (b) residues of PP/orgnoclays at various OBTN contents	108
5.8 XRD patterns of PP/orgnoclays (a) residue and (b) soluble fractions at various OBTN content	110
5.9 TEM micrographs of the 5 wt% PP/orgnoclays (a) composite, (b) residue fraction, and (c) soluble fraction	112

FIGURE	PAGE
5.10 Schematic representation of the morphology before and after solvent extraction	115

CHAPTER VI

6.1 Apparent shear stress of organobentonite-filled PP nanocomposites as function of apparent shear rate at varying OBTN concentrations	122
6.2 Apparent shear viscosity of organobentonite-filled PP nanocomposites as a function of apparent shear rate at varying OBTN concentrations	123
6.3 Apparent shear viscosity as a function of organobentonite concentrations at two constant shear rates (50 and 2000 s ⁻¹) and various temperatures	125
6.4 Apparent shear viscosity for 5 wt% of organobentonite-filled PP nanocomposites as a function of shear rates at various temperatures	127
6.5 Apparent shear viscosity of 5 wt% of organobentonite-filled PP nanocomposites as a function of reciprocal temperatures (1/T) at various shear rates	127
6.6 Extrudate swell (%) of unfilled and organobentonite-filled PP nanocomposites as a function of apparent shear rates (190°C)	134
6.7 SEM micrographs of the extrudates obtained at 210°C: (a) effect of the apparent shear rates (at 5 wt% OBTN filled); and, (b) effect of OBTN concentrations (at a fixed $\gamma_{app} = 400s^{-1}$)	135
6.8 Extrudate swell for 5 wt% organobentonite-filled PP nanocomposite as a function of temperature at various apparent shear rates	136

FIGURE	PAGE
6.9 Extrudate swell (%) of organobentonite-filled PP nanocomposites as a function of apparent shear stress (at 190°C)	136
CHAPTER VII	
7.1 Chemical structures of anionic surfactants guest molecules used for intercalation LDH-NO ₃	143
7.2 XRD patterns (a) and FTIR spectrum (b) of LDH-NO ₃ as compared with LDH-CO ₃	145
7.3 The effect of alkyl chain length (n_c) of sulphate surfactants on: (a) XRD pattern of the organomodified LDHs, (b) d-spacing and their arrangement between the LDH layers, and (c) average crystallite size	148
7.4 SEM micrographs of (a) LDH-CO ₃ , (b) LDH-NO ₃ , (c) LDH-C8, (d) LDH-C12, and (e) LDH-C20 at low and high magnifications	152
7.5 The FTIR spectra of (a) LDH-NO ₃ , (b) LDH-C8, (c) LDH-C12, and (d) LDH-C20	154
7.6 TGA/DTG curves of LDH-NO ₃ and the organomodified LDHs	155
7.7 Torque vs. time plot during melt mixing (a) and XRD patterns (b) of LDPE/organomodified LDHs nanocomposites	157
7.8 SEM micrographs of the nanocomposites (a) LDPE/LDH-C8, (b) LDPE/LDH-C12, and (c) LDPE/LDH-C20 at the low (3000X, left) and high (10000X, right) magnifications	159
7.9 TGA (a) and DTG (b) thermograms of LDPE/organomodified LDHs nanocomposites	161

FIGURE		PAGE
7.10	The dynamic (a) storage modulus, (b) loss modulus, and (c) loss tangent of LDPE/organomodified LDHs nanocomposites	165
7.11	(a) compared XRD patterns, (b) low and high magnification SEM images, and (c) $E'_{\text{composite}}/E'_{\text{pure matrix}}$ for 2.5 and 5 wt% of LDH-C12 nanocomposites	168

Abbreviations

BTC	N-alkyl dimethyl ammonium chloride salt
BTN	bentonite
CEC	cation exchange capacity
CTAB	Hexadecyltrimethyl ammonium bromide
DOEM	Methy di-[(partially hydrogenated) tallow carboxyethyl]- 2-dihydroxyethyl ammonium methyl sulfate
LDH	layered double hydroxide
LDH-C8	layered double hydroxide modified with 2-ethylhexyl sulfate/C8
LDH-C12	layered double hydroxide modified with dodecyl sulphate/C12
LDH-C20	layered double hydroxide modified with eicosyl sulfate/C20
LDPE	low density polyethylene
Mg-Al-LDH	magnesium-aluminium layered double hydroxide
MMT	montmorillonite
OBTN	organomodified bentonite
OMLS	organo-modified layered silicate, organosilicate
PCN	polymer-clay nanocomposite
PE-g-MA	polyethylene grafted maleic anhydride
PLSNs	polymer layered silicate nanocomposites
PP	polypropylene
PP-g-MA	polypropylene grafted maleic anhydride